Membrane surface morphology and fouling in filtration of high DOC water

Beata Gorczyca[1,*]

[1] University of Manitoba, Department of Civil Engineering, Faculty of Engineering Winnipeg, 15 Gillson St., MB R3T 5V6 Canada

Abstract. In Canada many potable water sources contain very high concentrations of Dissolved Organic Carbon (DOC), accompanied by a wide range of hardness. DOC reacts with chlorine used in water disinfection to form potentially carcinogenic chlorine disinfection by-products – Trihalomethanes (THMs) and haloacetic acids (HAAs). Dual membrane plants that combine microfiltration (MF) and ultrafiltration (UF)or nanofiltration (NF) can remove DOC and reduce THMs concentration, but these plants are prone to serious fouling of their UF or NF membranes. The objectives of our research are to study the mechanisms of UF/NF membrane fouling. We have determined various resistances of DOW Filmtech NF90 (flat sheet coupon), based on the resistance in series model. The experiments were conducted on a bench scale cross-flow membrane filtration unit (Sterlitech), using synthetic water with DOC of 11 mg/L and calcium hardness of 350 mg/L that represents typical surface waters in Manitoba (Canada). The results suggest that gel layer on the surface of the membrane has a significant contribution to the flux decline. Atomic Force Microscope (AFM) allowed for relatively inexpensive, non-destructive analysis of the surface area of the gel layer deposited on the membrane filter. The morphology of the gel layer was related to the gel layer resistance.

1 Introduction

In Canada many potable water sources contain extremely high concentrations of Dissolved Organic Carbon (DOC), often exceeding 20 mg/L. DOC reacts with chlorine used in water disinfection to form potentially carcinogenic chlorine disinfection by-products – Trihalomethanes (THMs) and haloacetic acids (HAAs). The high water DOC is the primary reason why ~70% of the potable water systems in the Province of Manitoba (Canada) exceed Federal and Provincial water quality standards for THMs of 100 ppb [1].

Dual membrane plants that combine microfiltration (MF) and ultrafiltration (UF) or nanofiltration (NF) can remove DOC and reduce THMs concentration, but these plants are prone to serious fouling of their UF/NF membranes.

In the Canadian Prairie region, the water DOC can range from 11-20 mg/L and water hardness can range from 50 mg/L-350 $CaCO_3$. The DOC and divalent cations (water hardness) can combine to promote rapid fouling and reduce UF/NF membrane life, leading to reduced performance and increased operation costs for the water treatment plants in this region.

American Membrane Technology Association (AMTA) recommends that to control fouling, water DOC must be reduced to below 2 mg/L prior to NF [2].

Our research indicates that, at most, 70% of DOC can be removed from Canadian Prairie waters, which is insufficient to bring it down to 2 mg/ [3-8]. Also, the reduction of one water quality parameter, namely DOC, does not guarantee prevention of fouling. This is because fouling depends on many water quality parameters and their interactions, specifically the interactions of DOC with metal ions, as well as membrane properties and operations. Therefore, the specific mechanism of fouling needs to be understood to control fouling of membranes operating on high DOC waters.

The highest natural water DOC currently reported in membrane filtration studies is 13 mg/L which is at the low end of the concentrations observed in many Canadian surface waters supplies [9-11].

Only literature dealing with wastewater treatment plant effluents has looked at membrane filtration of water with DOC higher than 13 mg/L. Therefore, one of the aims of this research is to address this knowledge gap by investigating the membrane fouling mechanisms in filtration of natural waters with extremely high DOC concentrations accompanied by high water hardness. Although the characteristics of wastewater effluents differ from natural waters; it may be possible, that some mechanisms of membrane fouling reported for membrane bioreactors may be applicable to organic rich natural waters [12-15].

* Corresponding author: Beata.Gorczyca@umanitoba.ca

1.1 Mechanism of membrane fouling

1.1.1 Membrane resistance

In membrane filtration the water flux decline is caused by a decreased driving force (transmembrane pressure) and/or an increased membrane resistance. Generally, several mechanisms have been postulated to explain why membrane resistance increases during filtration, including: a) loss of porosity due to membrane pore blockage b) formation of the fouling (gel) layer, and c) changes to the fouling layer structure [16,17-21]. Although the gel layer can usually be removed by physical cleaning, this type of resistance to filtration can sometimes represent more than 90 % of the total resistance for membrane filtration [22].

For MF and ultrafiltration membranes (UF) the modelling of membrane resistance to filtration is often based on classic filtration theory that includes Stokes', Darcy's and Carman-Kozeny's Laws [16, 22]. Although the transport of water through NF and some UF membranes is modelled typically using the thin-film model, it has been reported that combination of these two modelling approaches gives the best results [23].
According to filtration theory, for low feed concentrations and low transmembrane pressures, applicable to natural water filtration, the permeate flux can be modeled using the modified Hagen-Poiseuille equation [24]:

$$J = \frac{e\, dp^2 (P_T)}{32\, x\mu} \quad (1)$$

where:
J - permeate flux (volume permeate/(membrane area x time, L m^{-2} h^{-1})
e - membrane surface porosity
dp - mean pore diameter
P_T - net transmembrane pressure = (P_F-P_P)
P_F - feed pressure, P_P = permeate back pressure
X - pore channel length
μ - absolute viscosity of permeate.
The equation (1) can be simplified to Darcy's equation:

$$J = \frac{P_T}{(R_t)\,.\mu}\,[\mathrm{L}\cdot m^{-2}\,h^{-1}] \quad (2)$$

where:
R_t - the total resistance (m^{-1})

The resistances which can occur during a filtration process are membrane resistance (R_m), fouling resistance (R_f - consisting of reversible and irreversible fouling) concentration polarization resistance (R_p), and gel layer resistance (R_g) (Fig. 1). Assuming a resistance-in-series model, the total resistance is equal to the sum of all other resistances:

$$R_t = R_m + R_f + R_p + R_g \quad (3)$$

Determination of various membrane resistances using equation 2 requires measurements of the flux at different filtration pressure applied. The estimate of different membrane resistance can indicate the contribution of different mechanisms to total membrane fouling; however, it provides little information on the pattern of the events that leads to fouling. Eq. 2 as opposed to Eq. 1 does not contain information on membrane parameters directly related to mass transfer through the membrane such as porosity, pore diameters and pore channel length. In classical filtration theory these parameters are directly related to the mechanism of membrane fouling; but they can only be determined through by conducting a membrane autopsy.

The thin-film model is derived by equating the connective flux of the solute towards the membrane surface with the diffusive flux of the solute away from the membrane surface. Assuming this model, the flux through the membrane can be represented by [24]:

$$J = kln(\frac{Cgel}{Cretentate}) \quad (4)$$

where:
k - mass transfer coefficient (same units as flux J)
C - concentration of the solute.

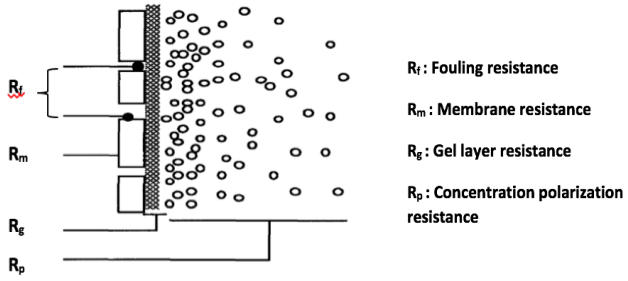

Fig. 1. Possible resistances against solvent transport through membranes [25].

1.1.2 Autopsy of membranes used in filtration of potable water sources

Properties of the virgin and fouled membrane can be studied through membrane autopsy. Current membrane autopsy protocols are based on methods used for foulants encountered within the food industry. Foulant analyses typically consist of: quantification of foulant dry density in mg/cm^2, determination of foulant composition, microbiological testing, and investigation of the foulant structure with Scanning Electron Microscopy. Most of these analyses are conducted on dried, fouled membrane. Yet, natural water membrane fouling layers, similarly to biofilms, are often composed of organic materials with extremely low density that can occupy significant volume, such as soluble microbial products [26]. Structures of such materials can change during drying, therefore, it can only be investigated through non-destructive, wet state analysis. Such analysis require the use of Confocal Scanning Laser Microscope (CSLM) or Small Angle Neutron Scattering (SANS) methods which are extremely expensive [17-21]. Atomic Force

Microscope (AFM) allows for relatively inexpensive analysis, non-destructive analysis of the surface area of the gel layer deposited on the membrane filter.

1.1.3 Relationship between external surface and internal structure of membrane fouling layer

Several techniques applied to study external structures of particle aggregates (flocs) and biofilms can be used, with modifications, to study the same properties in membranes. Biofilms can be represented as a group of compressed flocs immobilized on a substratum and several similarities between flocs and biofilms have been reported in the literature. It is difficult to describe the floc or biofilm structure using concepts of conventional geometry, due to "chaotic" distribution of particles inside these biomasses; however, floc and biofilm structure can be described in terms of fractal geometry [26-29].

Knowledge of the internal structure of the membrane fouling gel layer can provide information on the pattern of events that lead to its formation.

External surface morphology is closely related to the internal structure. For example, Fig. 2 shows that surface morphology of the gel layer formed by deposition of spherical particles will be quite different that that formed by deposition of fractal object (snow flakes in Fig. 2).

For example, the surface roughness, measured as the height difference between the peaks and valleys will be the same for the fouling layer formed with spherical particles. For deposits formed by the „snowflakes" the surface roughness will depend on the magnification (resolution) at which the measurements is conducted. Our earlier research on fractal structures of flocs suggest that deposit shown in Fig. 2 b may have lower resistance (higher permeability) than the Fig. 2 a [26-29].

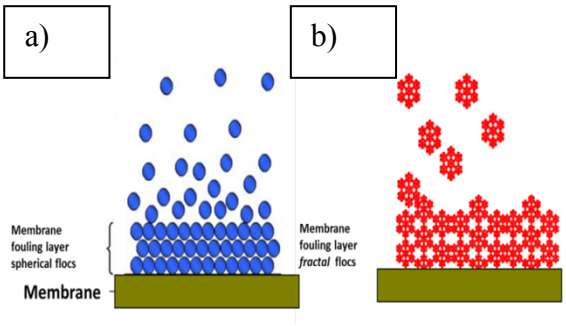

Fig. 2. Possible relationship between the structure of flocs and surface morphology of the membrane fouling layer.

The goal of our research is to obtain information on the mechanisms of fouling of UF/NF membranes used to filter high DOC and hardness surface waters. The specific contribution of this work is in linking the measurements of membrane resistance with the observation of changes in membrane surface morphology.

The long term goal of this research is to extend the life of membranes used to filter challenging surface waters, by understanding the fouling process.

2 Materials and methods

Morris Regional Water Treatment Plant (WTP), located in the Town of Morris (Manitoba, Canada), was upgraded in 2009 and officially opened in 2010 as a dual membrane treatment process. The upgrade converted a conventional lime/soda softening process to an integrated membrane treatment plant (microfiltration followed by nanofiltration). The schematic diagram of the water treatment plant in Morris is shown in Fig. 3.

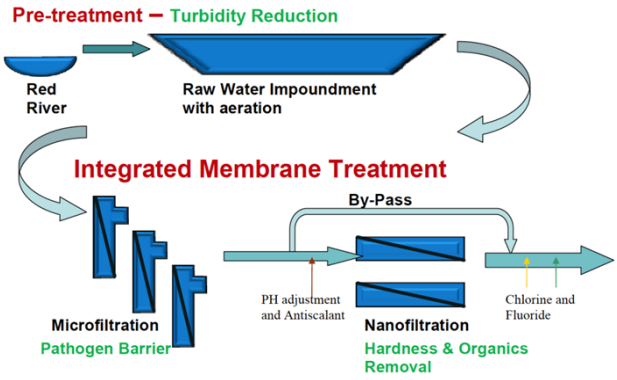

Fig. 3. Morris Regional Water Treatment Plant [30].

The plant operation is fully automated and runs 24 hours a day in summer (two nanofiltration skids run on alternate days) and 18-20 hours a day in winter depending on the demand at a constant present flow rate with a predetermined permeate flow. The membranes (Table 1) are periodically cleaned manually in place (every 2 – 3 months) using a solution of sodium hydroxide (NaOH) and citric acid as cleaning agents.

Table 1. Properties and of membranes used in the plant and the laboratory experiments.

Membrane Properties	Type of Membrane	
	TMG20-400C	NF90-400/34i
Membrane Material	Cross Linked Fully Aromatic Polyamide Composite	Polyamide Thin Film Composite
Molecular Weight Cut-off (Dalton)	< 200	90 - 200
Maximum Pressure (bar)	25	41
Maximum Temperature (°C)	45	45
NaCl Rejection (%)	99	85 – 95
Cross Flow Velocity (m/s)	0.374	0.34

The cleaning procedure is effective in restoring the permeability of the membranes and cleaning any reversible fouling occurred at the unit. However, due to high level of irreversible fouling, the NF membranes need to be replaced prematurely, which makes the treatment system uneconomical.
The NF membranes used in the water treatment plant are ultra low pressure Toray element for brackish water (TMG20-400C, Toray). The membrane specifications and operating conditions as specified by the manufacturer are presented in the Table 1. Fresh coupon of TMG20 using synthetic water was not available for the laboratory testing and a similar membrane NF90 DOW Filmtech was used (Table 1).

2.1 Laboratory determination of membrane resistances

Bench-top membrane filtration system was used to determine resistance of NF membrane. Feed water was pumped through a WEG Hydra-Cell constant flow pump forcing 7 L/min resulting in cross-flow velocity of 3.36 m/s. Water was pumped into a Sterlitech CF042D membrane filtration cell and ran in crossflow through the encased membrane coupon. Temperature of the water was carefully controlled through the heat exchanger. A flow diagram of the experimental setup can be seen in Fig. 4.

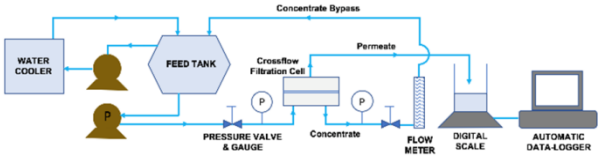

Fig. 4. Bench scale laboratory membrane filtration set-up [31].

The various membrane resistances were estimated using the resistance in series model (eq. 1 and 2). Synthetic water (Table 2) used in bench scale laboratory testing was prepared to mimic the DOC and hardness composition of the Red River water (Table 3).

The foulant accumulated on NF filters used to filter the Red River water (Manitoba) was reported to be composed primarily of hydrophilic neutral NOM fraction [31]. Based on that analysis, sodium alginate -an anionic polysachharide, which is a hydrophilic neutral compound was used to mimic natural water DOC. Calcium chloride, was used to impart hardness to the synthetic water. The concentration of the sodium alginate and calcium chloride used in the synthetic water was based on the concentration of Dissolved Organic Carbon (DOC) and Calcium hardness in Red River, as reported by Morris Plant (Table 3). NF90 membrane was compacted for 10 hours and fouled with synthetic water for 72 hours.

2.2 Membrane Autopsy

Gel layer external surface. The surface morphology of the foulant formed in the laboratory testing was observed using Atomic Force Microscope (AFM).

Table 2. Composition of synthetic water used in determination of membrane resistance.

Constituent	Formula	Molecular Weight	Concentration
Sigma Aldrich – Sodium Alginate	$(C_6H_7NaO_6)_n$	198 g/mol	11.6 mg/L as DOC
Calcium Chloride	$CaCl_2$	110.98 g/mol	350 mg/L as $CaCO_3$

Table 3. Quality of raw and treated water at the Morris Water Treatment Plant [30].

Parameter	Red River Water
pH	8.23
Alkalinity, Total (as $CaCO_3$), mg/L	261
Dissolved Organic Carbon (DOC), mg/L	11.6
Total Hardness, mg/L as $CaCO_3$	350
Calcium, mg/L	70.4
Magnesium, mg/L	42.2

A NanoScope IVa Controller (Veeco Dimension 3100) was used to show the change in foulant surface roughness during filtration. A 100μm^2 surface area was plotted in contact mode at a speed of 10μm/s. Three-dimensional surface images were collected for analysis.
Gel layer thickness. It was not possible to measure the thickness of the gel layer as the gelatinous foulant formed by synthetic water was difficult to section. However, the depth of the gel layer was measured on the fouled membrane colected from the Morris plant. Altough this membrane was fouled for much longer time that the coupons in the laboratory, it could provide some information on the relative thickness of the gel layer in comparison to the total membrane thickness. The membrane samples were carefully sectioned using sharp razor blade in wet condition and the best sections were used to view using Environmental Scanning Electron Microscope.

3 Results and discussion

3.1 Membrane resistance

The various resistances of the NF90 membrane determined in the laboratory scale apparatus are shown in Table 4. Total resistance of the TMG20 membrane collected from the plant was estimated in the laboratory to be 4.31E+14 m^{-1} and was comparable with the total resistance obtained for NF90 membrane. The difference between the values should be mainly due to the much longer filtration time applied at the WTP. The similarity of the total resistance of the membrane used in the laboratory study to the one collected from the plant validates the preparation of the synthetic water. The resistance results indicate that the fouling (R_f) and gel

resistance (R_g) are primarily responsible for the flux decline of the tested NF membrane. Analyses of the gel layer external surface was conducted to obtain more information on the pattern of event that have led to its formation.

Table 1. Various membrane resistances as determined in the laboratory.

Feed Water	Rm (10^{14} m^{-1})	Rt	Rp	Rg	Rf
Synthetic	1.17	3.88	0.55	0.97	1.19

3.2 Membrane Autopsy

3.2.1 Analyses of membrane surface morphology from Atomic Force Microscope (AFM) images.

In our earlier research, we have observed vastly different surface morphologies of in a number of DOW Filmtech NF membranes using AFM [15]. These membranes have different resistance which could be related to their different internal structures of the membrane and foulant, which in turn can be reflected in different surface morphology.

Changes in the virgin membrane surface morphology are certainly determined by the mechanism of fouling. The surface morphology of the two membrane gel layers shown in Fig. 5 is certainly different. The fouled membrane, which has higher resistance to flux, has markedly higher peaks than the clean membrane.

Fractal dimensions can provide information on the pattern of events leading to development of fouling layer. AFM profiles of NF90 virgin and fouled membrane are currently being analyzed using the box counting method [33].

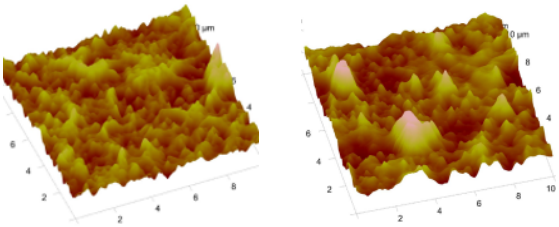

Fig. 5. DOW Filmtech NF90 membranes surface morphologies (left –clean, right-fouled).

3.2.2 Estimation of thickness of the gel layer

The images of cross-sections of the membrane collected and the plant is shown in Fig. 6. The cross-sectional images were very clearly identifying the smooth surface and depth of the gel layer on the membrane surface. Some cracks were visible on the top surface of the membrane samples, which might be a result of membranes drying and organic foulant flaking off. The estimated depth of the gel layer was about 27 μm and represented approximately 25% of the total thickness of the membrane.

Scale of the ESEM Image: 1 cm = 19.23 µm. Depth of Foulant (measured at three consecutive points) = 26.92 µm. Compacted Membrane Thickness = 107.69 µm.

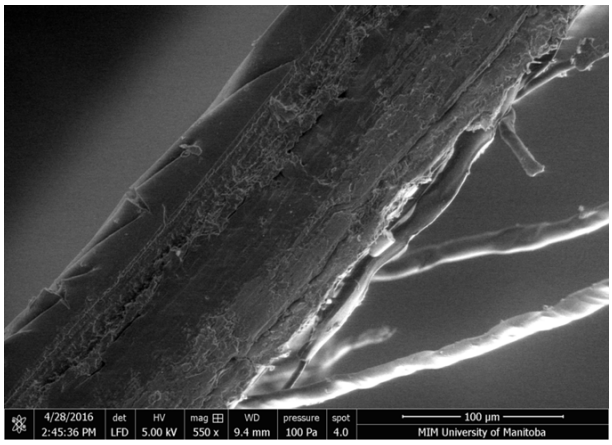

Fig. 6. Cross-section of nanofilter (TMG20) collected from Morris WTP [32].

4 Conclusions

The main operating cost of membrane filtration technologies lie in the fouling problem. In this research we have been investigating the mechanisms of fouling of NF membranes specific for filtration of challenging waters containing high concentration of DOC and carbonate hardness. The objective was to understand the mechanism of fouling to be able to control this process.

The resistance results indicate that irreversible and reversible fouling (Rf) and gel resistance (Rg), represented 55% of the total resistance of DOW Filmtech NF90 membrane fouled with high DOC and hardness water. Surface morphology and depth of the gel layer was analyzed. The gel layer on the fouled membrane fouled at the water treatment plant represented 25% of the total thickness of the membrane. The laboratory fouled membrane, with higher flux resistance, had different surface roughness than that of the clean membrane. Therefore, the external surface of the gel layer can be related to this layer resistance.

Nisha Jha, M.Sc. candidate, Dr.Zsolt Kiss, post-doctoral fellow, and Ian Moran an undergraduate student at the University of Manitoba were conducting membrane laboratory testing and some membrane autopsy analyses. The author would like to thank National Science and Engineering Research Council (NSERC) of Canada for supporting this research.

References

1. Manitoba Office of Drinking Water http://www.gov.mb.ca/conservation/waterstewardship/odw/public-info/general-info/compliance_data/
2. AMTA, 2017. American Membrane Technology Associaton. www.amtaorg.com

3. M. Sadrnourmohamadi, C. Goss, B. Gorczyca, Water Sci. Technol. Water Supply **13**, 3 (2013)
4. M. Sadrnourmohamadi, B. Gorczyca, Water Res. **73** (2015)
5. B. Gorczyca, J. Ganczarczyk, Wat. Qual. Res. J. Canada **37** (2002)
6. M. Sadrnourmohamadi, B. Gorczyca, Sep. Sci. Technol. **50** (2015)
7. M. Hooshyar, M. Winnipeg, Eng. Report, University of Manitoba, Civil Engieering (2015)
8. K. Brezinski, M. Sadrnourmohamadi, B. Gorczyca, West. Canada Water (2015)
9. Y. Bessiere, B. Jefferson, E. Goslan, P. Bacchin, Desal. **249** (2009)
10. N. Geismar, P. Berube, B. Barbeau, Desalin. Water Treat. **43** (2012)
11. H. Wray, R. Andrews, P. Berube, Desal. **330**, (2013)
12. F. Chen, et al., Water Res. **48** (2014)
13. J. Tian, M. Ernst, F. Cui, M. Jekel, Water Res. **47** (2013)
14. P. Le-Clech, V. Chen, T.A. Fane, J. Membr. Sci. **284** (2006)
15. B. Gorczyca, I. Moran, *IWA Spec. Conf. June 22-24* (2016)
16. M. R. Wiesner, J.M. Laine, *Water Treatment Membrane Processes* (New York: McGraw-Hill, Inc. 1996)
17. D. Antelmi, B. Cabane, M. Meireles, P. Aimar, *Cake Collapse in Pressure Filtration* (Langmuir 2001)
18. J. Madeline, M. Meireles, R. Botet, B. Cabane, Wat. Sci. Technol. **53**, 7 (2006)
19. J. Madeline, et al. Restructuring of colloidal cakes during dewatering (Langmuir, 2007)
20. C. Parneix, J. Persello, R. Schweins, B. Cabane, *How do colloidal aggregates yield to compressive stress?* (Langmuir, 2008)
21. B. Josson, J. Persello, J. Li, B. Cabane, *Equation of state of colloidal dispersions* (Langmuir, 2011)
22. K. Kimura, T. Maeda, H. Yamamura, Y. Watanabe, J. Membr. Sci. **320** (2008)
23. M. Elimelech, S. Bhattacharjee, J. Membr. Sci. **145** (1998)
24. M. Cheryan, Ultrafiltration and Microfiltration Handbook (Technomic Publishing Co. Inc., Pennsylvania 1998)
25. F. Meng, S.R. Chae, A. Drews, M. Kraume, H.S. Shin, F. Yang, Wat. Res. **43** (2009)
26. J. Ganczarczyk, *IWA Spec. Conf. on Biofilm Systems* (1996).
27. A. Vahedi, B. Gorczyca, Wat. Res. **45**, 2 (2011)
28. A. Vahedi, B. Gorczyca, Wat. Res. **46**, 13 (2012)
29. A. Vahedi A. B. Gorczyca, Wat. Res. **53** (2014)
30. Pembina Valley Water Co-op. Annual Reports. http://pvwc.ca/ (accessed April 23, 2017)
31. N. Svenda, B. Gorczyca, New Orleans, American Water Works Association (2014)
32. N. Jha, B. Gorczyca, Z. Kiss, *An. Conference, WCWWA, Saskatoon, Sept.19-22* (2017)
33. B. Kaye, Winheim: VCH Verlagsgesellschaft (1989)